The Time Course of the Probability of Transition Into and Out of REM Sleep

Alejandro Bassi, PhD[1]; Ennio A. Vivaldi, MD[2]; Adrián Ocampo-Garcés, MD, PhD[2]

[1]Department of Computer Sciences, Faculty of Physical and Mathematical Sciences, University of Chile, Santiago, Chile; [2]Laboratory of Sleep and Chronobiology, Program in Physiology and Biophysics, Faculty of Medicine, University of Chile, Santiago, Chile

Study Objectives: A model of rapid eye movement (REM) sleep expression is proposed that assumes underlying regulatory mechanisms operating as inhomogenous Poisson processes, the overt results of which are the transitions into and out of REM sleep.

Design: Based on spontaneously occurring REM sleep episodes ("Episode") and intervals without REM sleep ("Interval"), 3 variables are defined and evaluated over discrete 15-second epochs using a nonlinear logistic regression method: "Propensity" is the instantaneous rate of into-REM transition occurrence throughout an Interval, "Volatility" is the instantaneous rate of out-of-REM transition occurrence throughout an Episode, and "Opportunity" is the probability of being in non-REM (NREM) sleep at a given time throughout an Interval, a requisite for transition.

Setting: 12:12 light:dark cycle, isolated boxes.

Participants: Sixteen male Sprague-Dawley rats

Interventions: None. Spontaneous sleep cycles.

Measurements and Results: The highest levels of volatility and propensity occur, respectively, at the very beginning of Episodes and Intervals. The new condition stabilizes rapidly, and variables reach nadirs at minute 1.25 and 2.50, respectively. Afterward, volatility increases markedly, reaching values close to the initial level. Propensity increases moderately, the increment being stronger through NREM sleep bouts occurring at the end of long Intervals. Short-term homeostasis is evidenced by longer REM sleep episodes lowering propensity in the following Interval.

Conclusions: The stabilization after transitions into Episodes or Intervals and the destabilization after remaining for some time in either condition may be described as resulting from continuous processes building up during Episodes and Intervals. These processes underlie the overt occurrence of transitions.

Keywords: REM sleep regulation, REM sleep homeostasis, Mathematical models

Citation: Bassi A; Vivaldi EA; Ocampo-Garcés A. The time course of the probability of transition into and out of REM sleep. *SLEEP* 2009;32(5):655-669

THE CONCEPT OF BEHAVIORAL STATE, A FUNDAMENTAL NOTION FOR SLEEP NEUROPHYSIOLOGY, ASSERTS THAT THE BRAIN IS NORMALLY ORCHESTRATED into 1 of 3 discrete modes of functioning, each with its own principles of organization: wakefulness (W), non-rapid eye movement (NREM), and rapid eye movement (REM) sleep. The discrete character of behavioral states as stable configurations requires rapid transitions when switching from one state to another, a concept that has been illustrated by comparison with the flip-flop, a bistable electronic circuit.[1-3] The high variability observed in the duration of state bouts suggests that the timing of the switching process has a strong stochastic component. Although the overt expression of behavioral states is discrete and the transitions are abrupt, the likelihood of a transition into or out of a given state at any given moment could be conceived as being the result of a continuous underlying process. The unveiling of the processes that account for either permanence in a given state or a transition to another state may contribute to a better understanding of sleep mechanisms and functions.[4] The spontaneous sequential occurrence of the 3 behavioral states unfolding as a time series may be a useful source of information for that purpose.

REM sleep, a state that involves the activation of widespread areas in the brain,[5-7] has attracted much attention because of its phylogenetic and ontogenetic peculiarities, its circadian and homeostatic regulatory mechanisms, its proposed relationship with dreaming, and its relevance for many psychiatric and neurologic entities. This report is concerned with the occurrence and duration of REM sleep episodes and with the duration of the intervals between the end of one such episode and the start of the next one, which are here referred to, respectively, by the terms "Episode" and "Interval." Studies involving REM sleep usually determine its total amount and assess its recurrence pattern by stating the number of Episodes and some measure of central tendency and variability of the duration of Episodes and Intervals. The actual distribution of those durations can be more informative, since there are many very short and few very long Episodes.[8-11] The high variability in the length of Episodes and Intervals suggests a substantial degree of randomness in sleep regulation. Acknowledging this stochastic nature, it has been proposed that REM sleep analysis should be based on the modeling of the distribution of the duration of Episodes and Intervals.[12,13]

Our analysis emphasizes that duration of REM sleep Episodes and Intervals is the overt result of underlying processes that do not necessarily operate with the same time course. If the underlying process were the concentration of a given neurotransmitter in a key neural location, that process would not be expressed as a behavioral state in a straightforward deterministic manner. A state is not expressed because a process is above or below a fixed threshold; the process simply makes more or less likely either the permanence of the current state or the transition into a different state. The description of a hidden process must be inferred from actual data. The knowledge and characterization of that process should be relevant for understanding state tran-

Submitted for publication April, 2008
Submitted in final revised form January, 2009
Accepted for publication February, 2009
Address correspondence to: Ennio A. Vivaldi, Facultad de Medicina, Universidad de Chile, Independencia 1027, Santiago, Chile; Fax: 56-2-7776916; E-mail: evivaldi@med.uchile.cl

sitions and permanence. Two aspects are worth emphasizing: firstly, in a transition, a new state attempts to settle itself, but the previous state may linger and interfere with the consolidation of the new state; secondly, after a state is consolidated, processes may come into play that could undermine its permanence or build up a pressure to transit to a different state.

The main proposition of the present study is that the dynamics of underlying continuous processes that account for the likelihood of a transition at any given time after the beginning of an Episode or Interval can be statistically constructed. The distribution of the lengths of Episodes and Intervals should be understood as the result of those processes.

It must be noted that this approach markedly resembles what in biomedical literature is known as survival analysis. In survival analysis, there is a starting point, such as birth or the first symptoms of a disease, and an evolution where, at some point, a given outcome occurs. It makes sense at any point in time to ask about the likelihood that the outcome occurs at that precise time. This instantaneous measure is the hazard function, also called failure rate or instantaneous death rate,[14] that describes the dynamics of the underlying process. Knowing these dynamics, answers are found to questions such as what is the probability that, given the fact that the outcome has not yet occurred after a given time, it will occur in a given consecutive time lapse. Rounding up the analogy, "instantaneous death rate" becomes "instantaneous transition rate" for exiting a REM sleep episode or exiting an Interval. According to our previously outlined rationale, a histogram of the distribution of age at death is limited to the results of a process; what should matter is the underlying process itself that has to do with endogenous and environmental aspects of human development and how they relate to the greater or lesser likelihood of occurrence of lethal diseases or other causes of death at any given age.

Stochastic events are usually modeled by a Poisson process characterized by a single parameter, usually called λ, which is technically called *intensity*, and corresponds to the expected rate of event occurrence. In homogeneous Poisson processes, λ is constant, and the result is an exponential distribution of time Intervals between events. In inhomogeneous Poisson processes, λ may vary linearly, as is the case of the Rayleigh distribution,[15] in which λ increases with time. Alternatively, if no assumption is made on constancy or linearity of the modulation of the rate of occurrence, a nonparametric approach must be followed to assess how λ changes in time. Furthermore, since we deal with discrete epoch data, λ can be approximated by normalizing the probability of occurrence of the transition event in an epoch by the duration of the epoch. The estimation of λ can then be achieved by the use of standard statistical methods such as logistic regression.

The overt dynamics of REM sleep occurrence involves the tendency to enter and exit REM sleep. The purpose of the present study was to determine the time course of these 2 processes that are here designated, respectively, as REM sleep propensity and REM sleep volatility. REM sleep propensity is quantified by the rate of occurrence of the NREM-sleep-to-REM-sleep transition process as an Interval evolves and represents the likelihood of entering a new Episode. REM sleep volatility is determined by the rate of occurrence of the out-of-REM transition process as an Episode evolves and is related to the likelihood of exiting a REM sleep episode. Since transitions into REM sleep normally occur only from NREM sleep, a third variable must be defined, REM sleep opportunity, which is the probability of NREM sleep occurrence throughout an Interval.

Finally, the modeling of REM sleep occurrence in terms of its propensity and volatility is examined in the context of its 24-hour distribution; its relationship to NREM sleep and W; and its short-term homeostasis, ie, the fact that longer Episodes tend to be followed by longer Intervals.[10,12,13,16-20]

METHODS

Sleep Recordings and Scoring

Data were obtained from 16 male Sprague-Dawley rats. Continuous recordings of 3 consecutive days from each rat were analyzed. Experiments conformed to the policies of the American Physiological Society. The animals weighed 250 to 300 g and were previously implanted with chronic electrodes under intraperitoneal chlornembutal 3 mL/kg anesthesia. After surgery, rats were housed in a 30x30x25 cm cage, placed within an 80x80x80 cm sound-isolated cube, under a light-dark schedule with lights-on, approximately 500 lux, from 08:00 to 20:00 local time. Throughout this report, time of day is indicated as zeitgeber time (ZT), so lights go on at hour 00 and off at hour 12. At least 10 days were allowed for recovery from surgery and acclimatization to the recording environment. More detailed information can be found elsewhere about the recording conditions, the computer-based data-acquisition system, and the algorithm used for state diagnosis.[21-23]

The data-acquisition program sampled 2 cortical, 1 hippocampal, and 1 neck muscle channel every 2 milliseconds searching for relevant graphoelements: single delta waves (1-4 Hz), trains of 3 consecutive sigma waves (11-16 Hz), trains of 8 theta waves (4-8 Hz), and muscle spikes or movement artifacts. The software quantified and stored the amount of detected elements in each successive 15-second epoch. Epochs were assigned to NREM sleep, REM sleep, or W by means of an off-line automated state scoring procedure that related the actual values of the 4 variables in a given epoch with their respective thresholds. If the muscle signal was above its threshold, the epoch was ascribed to W. If theta was above its threshold, the epoch was assigned to REM sleep. On the other hand, if either delta or sigma or both were above their thresholds, it was considered NREM sleep. If no variable was above threshold, the epoch was assigned to W. Each day of recording was thus summarized into a state-by-epoch array containing 5760 assignments. The automated detection procedure was manually corroborated by periodic visual inspection of raw data. Typical agreement of automated and visual scoring was around 90%. A REM sleep episode was considered to start at a transition from NREM sleep to REM sleep. An Interval was considered to start at a transition from REM sleep to either NREM sleep or W. For clarity, we will use the term *episode* to refer to only an uninterrupted sequence of REM sleep epochs and will use the term *bout* to refer to a sequence of uninterrupted NREM sleep epochs within an interval.

Since state distributions throughout the 12:12 L:D cycle are strongly modulated, the 24-hour database was subdivided into 3 segments. Boundaries were chosen based on results from a previous report[20] on the hourly distribution of the 3 states and

of a subset of NREM sleep ("delta-rich NREM sleep") consisting of its upper quintile in each day that had the highest content of delta waves. NREM sleep and W had step distributions with the higher level in the dark or light phase, respectively, whereas REM sleep had a sinusoidal distribution with a summit in the second half of the light phase. These results will be later corroborated here in Figures 1 and 3. Delta-rich NREM sleep had a remarkably sharp modal distribution around the first hour of the light phase. If a state were distributed evenly throughout the day, each hour would contain 1/24 or 4.16% of the daily total. The fraction of daily total delta-rich NREM sleep exceeded 12% in the first hour of the light phase, and the sum of the last hour of the dark phase and the first 2 hours of the light phase exceeded 30% of daily total. That fraction fell very quickly afterward. REM sleep, on the other hand, rose from near 4% to near 5 % from the third to the fourth hour of the light phase and increased rapidly. These facts suggested that ZT 03 would be an appropriate boundary between the delta-rich NREM sleep segment and the high REM sleep incidence segment. REM sleep hourly fraction of the day total was maintained above 4% until the first hour of the dark phase. Nevertheless, because of some peculiarities of REM sleep expression[20,24] and of its short-term homeostasis[25] that occur at the beginning of the dark phase, it seemed prudent to set the REM-sleep-rich segment boundary at ZT 11. All facts considered, the 3 time segments were defined as ZT 23-03, ZT 03-11, and ZT 11-23. A total of 6871 cycles were detected in the 48 days examined. The ZT 23-03 segment contained 2811 cycles, the ZT 03-11 segment contained 3404 cycles, and the ZT 11-23 segment contained 656 cycles.

Discrete Time Approximation for Inhomogeneous Poisson Processes

A Poisson process is a stochastic system in which discrete events take place independently so that the probability of observing N events over a time interval of length t obeys the Poisson distribution:

$$P\{N(t) = n\} = \frac{(\lambda t)^n}{n!} e^{-\lambda t}$$

It is worth noticing that, for data such as ours in which discrete epochs are assigned to a given state, whenever a state transition event occurs, the system ends up in a setting in which the same transition cannot be repeated in the same epoch, and, hence, only the first event occurrence makes sense (n = 1).

The parameter λ defines the intensity or rate of occurrence of the process. If the rate of occurrence is constant, which is the standard assumption, it can be estimated from given data as the mean number of events per time unit or as the inverse of the mean length of the intervals between events:

$$\lambda = \text{E[number of events per time unit]} = \text{E[interval length]}^{-1}$$

The time interval between the occurrences of events, ie, the time for a transition event to take place, follows then the exponential distribution:

$$P\{\text{time between events} > t\} = e^{-\lambda t}$$

However, if the underlying Poisson process is assumed to be inhomogeneous, the rate of occurrence of the triggering of a transition to state s at time t becomes a time variant parameter $\lambda_s(t)$. This parameter can not be estimated in the simple way explained above and must be locally determined as:

$$\lambda_s(t) = \lim_{\Delta t \to 0} \frac{P\{\text{observing a transition to } s \text{ in } [t, t+\Delta t]\}}{\Delta t}$$

A discrete time approximation to $\lambda_s(t)$ can be constructed based on the fact that, according to the Poisson assumption, if Δt is small enough, the probability of observing more than 1 event in an interval $[t, t+\Delta t]$ is very low. The probability of detecting a transition to state s at time t considering an observation window of length Δt can then be reliably approximated by:

$$P\{\text{observing a transition to state } s \text{ at time } t\} = \lambda_s(t)\Delta t$$

Our database is generated by a scoring procedure that assigns each consecutive 15-second epoch of recording to a given state. Hence, we start from a sequence of discrete epochs of equal duration Δt, each labeled with a state diagnosis. In this sequence, the probability of detecting a transition to state s at time t is the same as the probability of observing s at epoch $e(t) = [t, t+\Delta t]$ under a condition $c(t)$ appropriately defined for t. The problem of estimating $\lambda_s(t)$ can then be solved using:

$$\lambda_s(t) = \frac{P\{\text{observing state } s \text{ at } e(t) | c(t)\}}{\Delta t}$$

Frequency-based Probability Estimation

A method directly based on the frequency of events can be used to estimate the observation probabilities. For example, the probability of observing state b given a previous stay in state a totalizing n epochs is calculated from the data as:

$$P\{b | n \text{ epochs in } a\} = \frac{\#\text{ sequences totalizing } n\ a\text{'s followed by } b}{\#\text{ sequences totalizing } n\ a\text{'s}}$$

The total number of epochs for a is determined from the onset of state a. If the time elapsed is measured likewise, the rate of occurrence of the triggering of the transition to b can be estimated using:

$$\lambda_b(n\Delta t) = \frac{P\{b | n \text{ epochs in } a\}}{\Delta t}$$

The estimation above is defined for discrete time increments, but it can also be interpolated if a continuous result is desired. A weakness that this approach may find is that the data are often too sparse to provide smooth and statistically sound probability estimates.

Model-based Probability Estimation

The estimation of observation probabilities can be achieved using logistic regression. The data consist in a set of pairs

$D = \{(x^i, o^i)\}_{i = 1,\ldots,K}$, where x^i is a vector that represents an observation condition and o^i is a value that defines the observation itself: 1 if the studied case is observed, 0 if not. The logistic regression model $M(x)$ is a function of the observation condition x. Its output represents the probability estimation for the observation under the requested condition.

To enhance the quality of the results and provide confidence intervals, a *bagging* or *bootstrap aggregation* technique can be advantageously applied.[26] The original data set is resampled using a random selection with replacement to generate L different data sets D^j. For each of them, a logistic regression model $M^j(x)$ is obtained. Finally, an aggregated model is constructed averaging the results of the L models thus obtained. The standard deviation of the L results represents the expected variability of the method with different data sets. It can be used to estimate the confidence interval of the result of the aggregated model for the given condition x.

Studied Models

The observation conditions considered in this work are represented by, firstly, the time elapsed from the beginning of the current REM sleep episode or Interval; secondly, for the time of day; and, thirdly, when dealing with short-term homeostatic effects, by the duration of the Episode preceding the current Interval or of the Interval preceding the current Episode. REM sleep opportunity and REM sleep propensity are evaluated from the onset of the ongoing Intervals, whereas REM sleep volatility is evaluated from the onset of the ongoing Episode. Three basic models were defined:

- $O(ti)$ for REM opportunity, where ti is the time elapsed since the beginning of the Interval,
- $P(ti)$ for REM propensity, also dependent of ti, and
- $V(te)$ for REM volatility, where te is the time elapsed since the beginning of the ongoing REM sleep episode.

These models account for the dynamic evolution of the respective variables. The estimation of $O(id)$ is used directly. In contrast, the estimations of $P(ti)$ and $V(te)$ are normalized by Δt, as explained above, and are expressed as events per minute. To determine the influence of the hour within the light:dark cycle (h) over the results, 3 enlarged models were defined, 1 for each case, $O_h(ti,h)$, $P_h(ti,h)$, and $V_h(te,h)$, where h represents the hour of the day. The influence of the duration of previous REM sleep episode (dpe) or Interval (dpi) was taken into account by defining the enlarged models $O_{dpe}(ti,dpe)$, $P_{dpe}(ti,dpe)$ and $V_{dpi}(te,dpi)$. Propensity was also examined in terms of the W and NREM sleep content within an Interval, of the time course of a NREM sleep bout, and of the duration of the Interval that preceded such NREM sleep bout.

Basic models are implemented as a logistic function applied to the linear combination of the hyperbolic tangents of 10 cubic polynomials of a given input variable. The enlarged models are similar except that quadratic forms are used instead of cubic polynomials. The input of the model, x, is a vector of 1 component for $O(ti)$, $P(ti)$, and $V(te)$; of 2 components for $O_{dpe}(ti,dpe)$, $P_{dpe}(ti, dpe)$, and $V_{dpi}(te\ dpi)$; and of 3 components for $O_h(ti,h)$, $P_h(ti,h)$, and $V_h(te,h)$. In the latter case, 3 components are needed because the parameter h is first expanded to 2 auxiliary values $hs = \sin(2\pi h/24)$ and $hc = \cos(2\pi h/24)$ before computing the output of the models. Input variables ti, te, dpi, and dpe are log scaled, providing further smoothing for larger values.

To train the models, first a data set was generated for each case from the original state sequences provided by the data-acquisition program. Next, each data set was resampled to create 25 versions with the same size. Then, for each case, 25 different trained models were obtained using the 25 resampled data sets to adjust the model variables. Finally, the trained models were aggregated to estimate the results.

RESULTS

The results deal with the process of going into REM sleep as modeled by the evolution of opportunity and propensity throughout an Interval and with the process of going out of REM sleep as modeled by the evolution of volatility throughout an Episode.

Figure 1 displays the hourly amount of W, NREM sleep, and REM sleep throughout the 3-day recordings. Figure 2 displays the time course of opportunity and propensity through an Interval and of volatility through an Episode. Figure 3 deals with the modulation of those variables throughout the 12:12 L:D schedule. Figure 4 reappraises propensity considering specifically the NREM sleep bout before the transition to REM. Figure 5 compares propensity with NREM sleep to W transition rate. Finally, Figures 6 to 8 refer to short-term homeostasis by examining the influence of the previous episode on opportunity and propensity and of the previous interval on volatility.

Most computations involved up to minute 4.0 of REM sleep episodes and minute 20.0 of Intervals. Those limits included 99.6% of Episodes and 90.3% of Intervals from the total of 6871 cycles detected. The distributions of both Episodes and Intervals had modes at 1-epoch duration, the modal frequency accounting for 47.7% in the case of Episodes and for 16.2% in the case of Intervals.

The hourly averages of the incidence of the 3 states in the 16 rats throughout the 72 recorded hours are displayed in Figure 1. The overall amount of each state as a fraction of total recorded time is 51.8% for W, 39.4% for NREM sleep, and 8.8% for REM sleep. Approximately two thirds of W occurs in the light phase and two thirds of NREM sleep occurs in the dark phase. The 8 hours of the ZT 03-11 time segment contain 50.6% of total time spent in REM sleep. The average hourly amount of REM sleep is 2.6% in the 4 hours of ZT 23-03, 6.3% in the 8 hours of ZT 03-11, and 3.2% in the 12 hours of ZT 11-23.

Time Course of Opportunity and Propensity Through an Interval and of Volatility Through a REM Sleep Episode

Figure 2 presents 3 columns of panels that display data corresponding to the time segments ZT 03-11, 11-23, and 23-03. The upper row represents Opportunity. The next 3 rows represent Propensity as a function of, respectively, the elapsed time in the Interval, its specific content of NREM sleep, and its specific content of W. The bottom row represents Volatility. Each panel shows the output of the aggregated model with its error range and the results calculated directly from actual frequencies. It can be noted that the output of the model follows well the actual frequencies and that the model achieves, as intended, a smoothing effect.

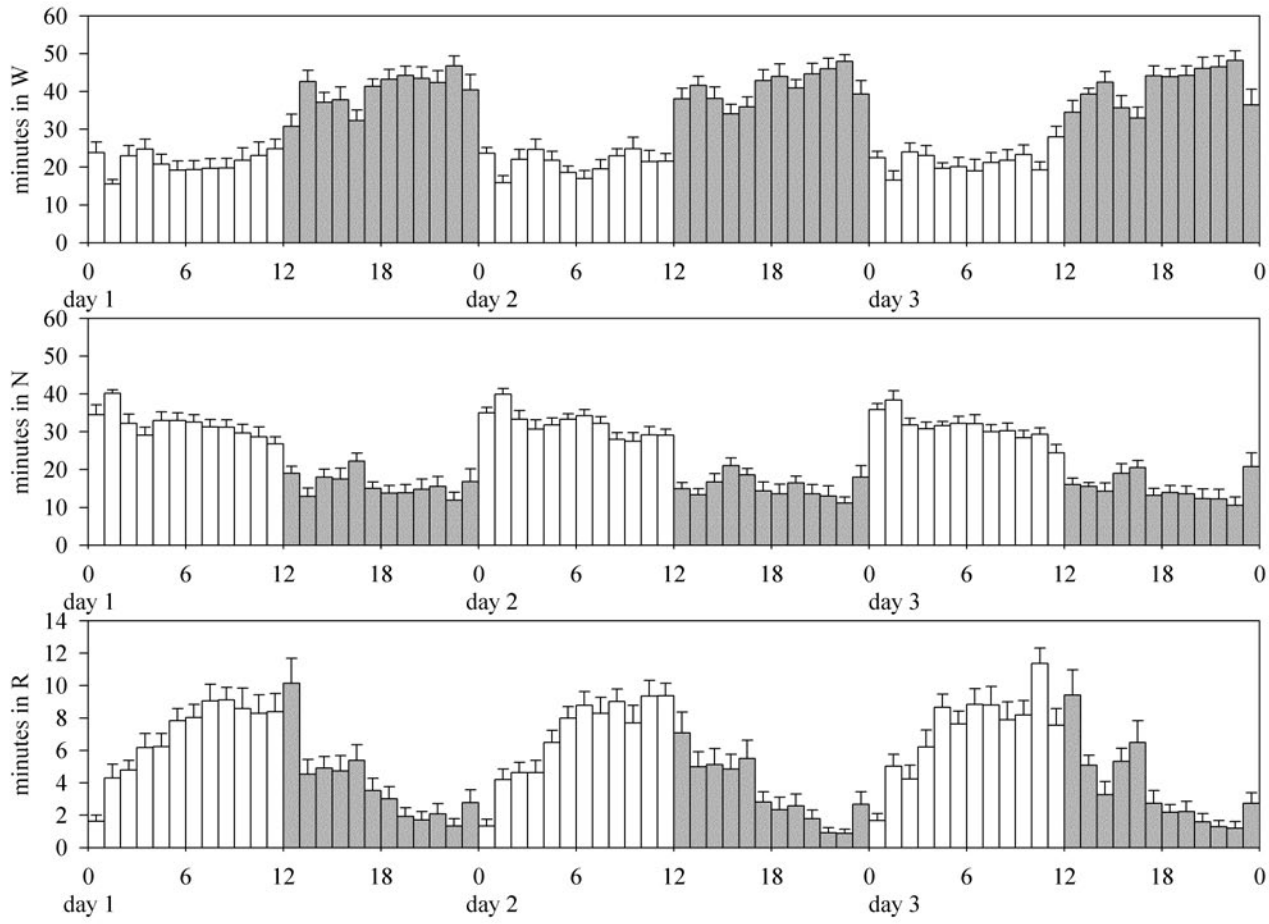

Figure 1—Average and standard error of the mean of minutes per hour spent in wake (W), non-rapid eye movement (NREM) sleep, and rapid eye movement (REM) sleep throughout the 3-day recordings. The 12:12 L:D cycle is highlighted by the bar colors.

We will first concentrate on the panels of the column corresponding to time segment ZT 03-11. The upper panel displays REM sleep opportunity or, as already stated, the probability of NREM sleep occurrence as a function of the time elapsed since the beginning of the ongoing Interval. The NREM sleep probability is 0.28 in the first epoch of the Interval, indicating that out-of-REM transitions occur mainly toward W. Afterward there is a fast rise in NREM sleep so that its probability reaches 0.74 at about 4 minutes after the beginning of the Interval, followed by a sustained decay for the rest of the 20-minute observation span.

Propensity falls in about 3 minutes to approximately one fifth of its initial value. Volatility falls in about 1 minute to approximately one third of its initial value. After the nadir, the behavior of propensity and volatility differ. While the former shows only a modest increase, at least in these first 20 minutes, the latter displays a conspicuously ascending phase. The third-row panel displays propensity as a function of cumulated NREM sleep content in the Interval, and the fourth row panel that of W content. The just mentioned increase in propensity occurs in the former, not in the latter.

Two of the variables present noticeable differences when the other time segments are compared with ZT 03-11. Opportunity displays a faster decay in ZT 11-23 and a very slow decay in ZT 23-03. The increase in propensity is less evident in ZT 11-23 and is absent in ZT 23-03.

Modulation of Opportunity, Propensity and Volatility Through the 12:12 L:D Schedule

Figure 3 displays, as 3D mesh plots, hourly values of opportunity and propensity through an Interval and of volatility though an Episode. Opportunity in Figure 3A displays 3 partitions: a ridge corresponding to the last hour of darkness and first 3 hours of light, a higher plateau for the rest of the light phase, and a lower one for the dark phase. Propensity at the beginning of the interval displays a marked modulation with a strong rise through the light phase and a nadir some 9 hours into the dark phase. The shape of the curve changes through the Interval. The initial high level of propensity observed during the light phase diminishes more rapidly than the shoulder observed at ZT 16 at the beginning of the Interval. The modulation of volatility is also much more pronounced at the beginning of the Episode, being highest at the end of the dark phase and lowest at the end of the light phase.

Propensity Through a Bout of NREM Sleep and its Interplay With Preceding Interval Duration

So far, we have examined propensity in terms of the variables Interval, cumulated NREM sleep, and cumulated W. To assess an eventual specific NREM sleep effect, the variable Interval is obviously inadequate. The variable "cumulated NREM sleep

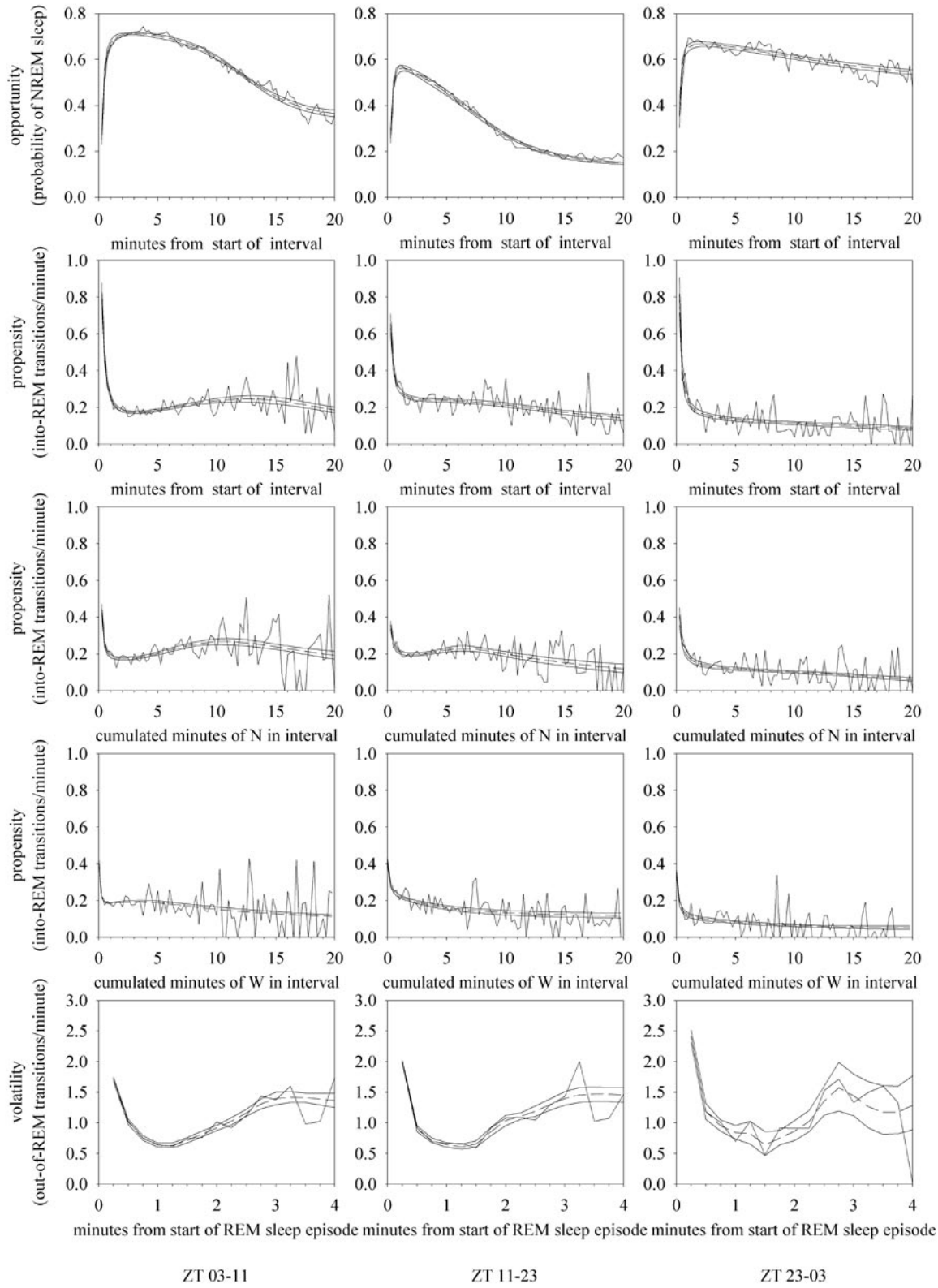

Figure 2—The dynamic courses of opportunity and propensity throughout an Interval and of volatility throughout a rapid eye movement (REM) sleep Episode are displayed for 3 time segments in which the 24-hour data is divided. The 3 columns display data for time segments ZT 03-11, ZT 11-23, and ZT 23-03. The first of the 5 rows display data for opportunity; the second to fourth for propensity as a function of, respectively, Interval, cumulated non-rapid eye movement (NREM) sleep in Interval, and cumulated W in Interval; and the fifth row for volatility. Each panel shows the output of the aggregated model (dashed curve) within a 1-standard deviation span (smooth solid curves). The results of the model can be compared with those of frequency-based estimation (broken solid curve). Opportunity is measured as NREM sleep probability, a value between 0 and 1 that is the complement of the probability of being awake at any point of the Interval. Propensity and volatility are measured, respectively, as the rate of occurrence of the into-REM and of the out-of-REM transitions expressed as events per minute.

within the Interval" is also unsatisfactory, since it is equally affected by NREM sleep occurring earlier or later during an Interval. These considerations led to the analysis presented in Figure 4, in which propensity is expressed as a function of 2 variables, the ongoing NREM sleep bout and the time within the interval in which that bout starts. The latter variable corresponds to the preceding interval or the time lapse from the end of the last REM sleep episode to the beginning of the NREM sleep bout being examined. The analysis was performed separately for the 3 time segments. Results are presented in Figure 4 as 3D mesh plots at left and as 2D panels at right displaying selected sections along the 'preceding Interval' axis.

In Figure 4A, propensity starts at a high initial level, a rate of 0.80. In the mesh plot, there is an asymmetry in the drop of the first line of each axis. As we move along the NREM sleep bout lacking a preceding interval, propensity equals 0.50, 0.40, and 0.31 at minute 0.5, 1.0, and 2.0 into the NREM bout. As we move along longer preceding intervals, propensity equals 0.22, 0.12, and 0.08 when the bout starts at 0.5, 1.0, and 2.0 minutes into the Interval.

The first panel in the 3 time segments corresponds to a section at preceding Interval equaling 0, a NREM epoch immediately following a REM sleep episode, so the starting point in each of them is the same as in the corresponding graphs of the second row of Figure 2. In the next panel, corresponding to a preceding interval of 0.5 minutes, there is no longer a high starting point with the subsequent flattening of the curves. The next panel corresponds to a preceding interval of 3 minutes and shows a remarkable change, since the curves start from the lowest value and increase for approximately the first minute. From then on, the graphs of time segments ZT 03-11 and ZT 11-23 differ from that of ZT 23-03. In the former time segments, propensity goes through a plateau and later displays a second rising phase. The same pattern is observed after 6, 12, and 18 minutes of preceding intervals. The plateau being somehow more sustained, some 4 minutes, in ZT 03-11 and somehow earlier, some 2 minute, in ZT 11-23. On the other hand, in time segment ZT 23-03, after the initial 1-minute increase, the curve turns down, reaching levels close to 0.

For a better judgment of the behavior of propensity through a NREM sleep bout, we decided to compare it with the rate of occurrence of transitions to W, since, as a NREM sleep bout evolves, there are 2 possible ways for it to end: in a transition to REM sleep or by waking up. Figure 5 is identical in analysis and graphic displays to Figure 4, but, instead of measuring propensity to REM sleep, it refers to transition from NREM sleep to W as a function of the ongoing NREM sleep bout and the time within the interval in which that bout starts. The difference between the 2 cases is remarkable. Note that REM sleep propensity starts at its highest level at the beginning of the NREM sleep bout only when there is no preceding interval to that bout. The behavior of the rate of transition from NREM sleep to W is remarkably different, always displaying its highest level at the beginning of the NREM sleep bout with its following descent being more or less patent. In a few cases, such as the panels of 6, 12, and 18 minutes of preceding interval in ZT 03-11, some rebound is observed in the NREM sleep to W transition rate after it reaches its lowest value approximately 1 minute into the bout.

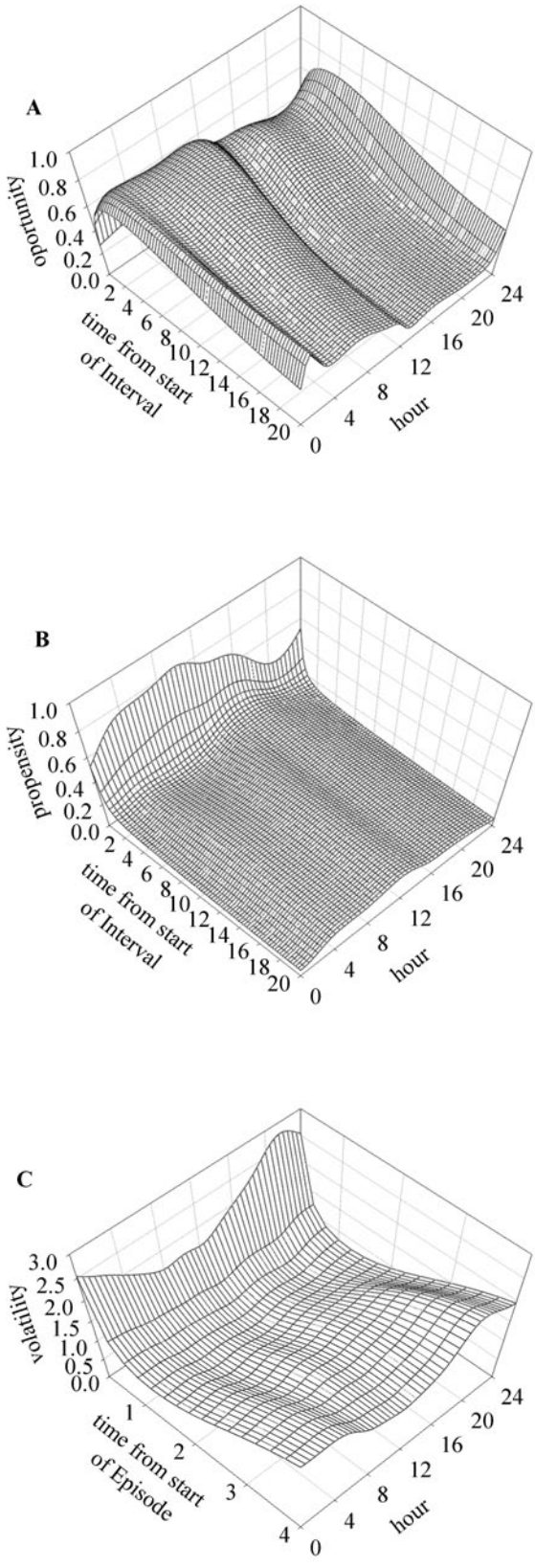

Figure 3—The dynamic courses of **A.** opportunity and **B.** propensity throughout an Interval and of **C.** volatility throughout a rapid eye movement (REM) sleep Episode are displayed in 3D mesh plots that add as a second modulating variable the time-of-day, where 0 corresponds to lights-on time.

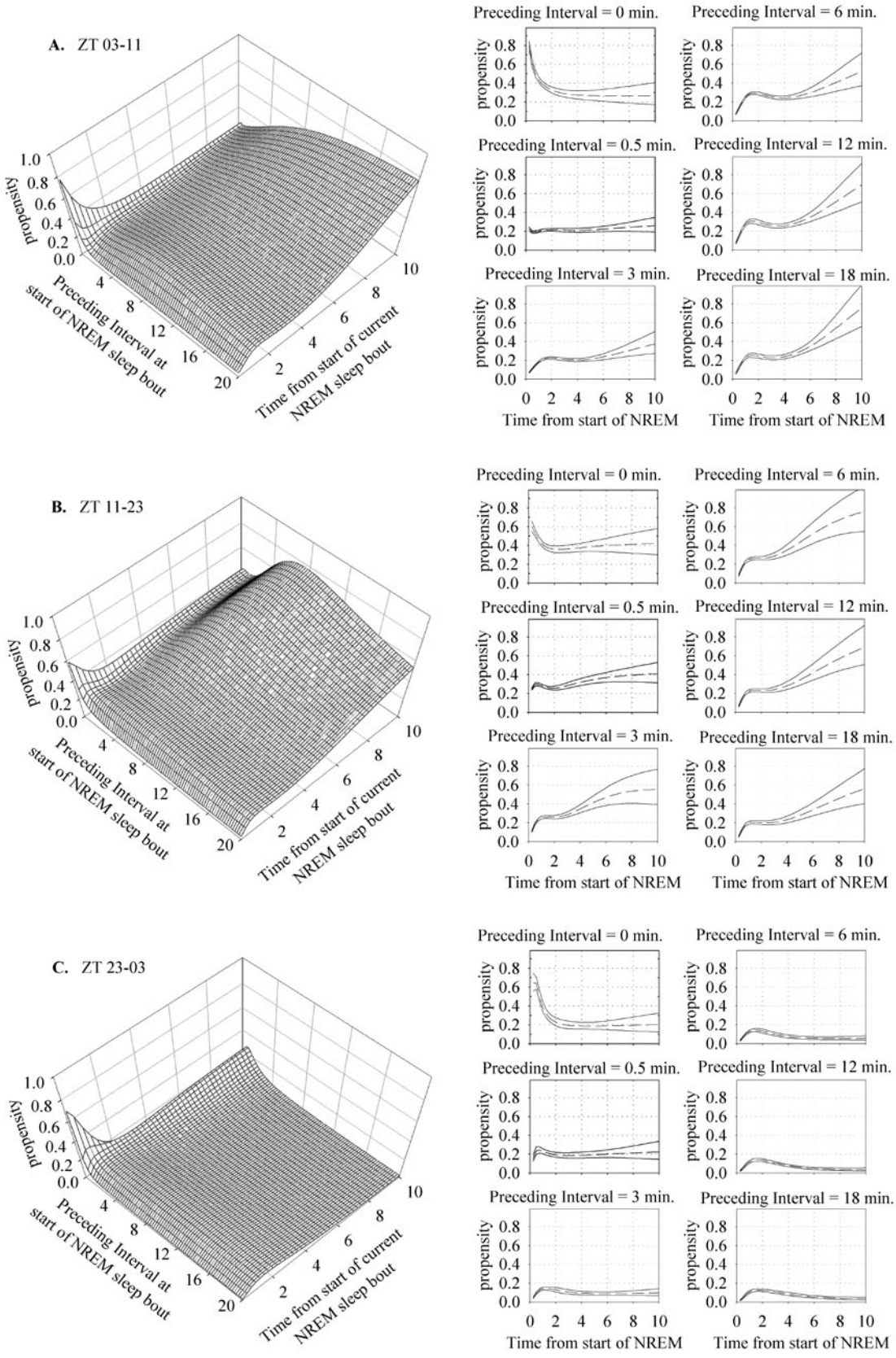

Figure 4—The three 3D mesh plots correspond to time segments of 24-hour data: **A.** 03-11, **B.** 11-23 and **C.** 23-043 and display the dynamic course of propensity through a given non-rapid eye movement (NREM) sleep bout adding as a second modulating variable the time at which the NREM bout began after the Interval started. The 2D panels at the right of each 3D mesh plot are cross sections displaying the modulation of propensity as a function of time from the start of the NREM bout at 6 different times elapsed from the beginning of an Interval and the start of the NREM sleep bout being examined.

Modulation of Opportunity and Propensity Curves by Previous Episode Duration

The dynamics of opportunity as a function of the duration of the previous REM sleep episode in ZT 03-11 is presented in Figure 6. The pattern of a sharp increase and slow decrease in opportunity throughout the ongoing Interval observed in Figure 2 can now be shown also as a function of the length of the previous Episode. The highest value of opportunity moves toward later times within the Interval when previous Episodes are longer, as indicated by comparison of the 3 panels of Figure 6B. Shorter previous Episodes, as compared with than longer ones, tend to be followed more by NREM sleep, as can be seen in the upper panel of Figure 6C.

The time course of propensity throughout an Interval as a function of the length of the previous REM sleep episode is displayed in Figure 7. The 3 panels of Figure 7C indicate that the overall time course of propensity displayed by the corresponding panel of Figure 2 (first column, second row) is the resultant of different profiles. When the previous Episode is very short, the starting point of the curve is lower and the descent is shorter. When the previous Episode is very long, an intense and sustained dip is observed. Note that, in the lower panel of Figure 7C, where very long preceding Episodes are represented, the dip is so marked that it seems practically impossible to go back to REM sleep in the time window spanning from 1.0 to 5.0 minutes from the start of the Interval.

The first panel of Figure 7D illustrates propensity as a function of previous REM sleep episode length at time 0.25 minutes after the start of the Interval and indicates that propensity is lower for very short and very long previous Episodes, attaining a plateau when the previous Episode had a length between 1.0 and 2.0 minutes.

In the last 6 panels of Figure 7D, the scale of propensity has been changed to highlight the evolution of this variable from minute 2.5 to 15.0 of the Interval. The sequence of panels illustrate that, at 2.5 minutes after the start of the Interval, the propensity curve shows a sharp descent so that, for example, a 1.5-minute previous Episode is quite effective in keeping a low propensity. As the Interval evolves, the shape and slope of the curve change. Note that the all 6 curves start from a similar level, ie, a very short previous Episode is followed by a high propensity that does not vary along the Interval; on the other hand, longer Episodes will have an impact on propensity, an impact that will fade as the Interval evolves.

Modulation of the Volatility Curve by Previous Interval Duration

Figure 8 displays the dynamic course of REM sleep volatility as a function of the previous Interval duration. The influence of the previous Interval, as seen in Figure 8B, is mostly noticeable at the very start of the ongoing Episode when the initial volatility is much higher after longer Intervals with a subsequent a sharper drop. The initial volatility is lower for very short Intervals, and the descent that follows is quite modest, an effect that can be confirmed in the upper panel of Figure 8C. The next 2 panels indicate that, afterward, volatility is largely independent from previous Interval duration.

DISCUSSION

The sleep-wake cycle presents itself as a sequence of discrete states. In transitions from one state to another, neural reorganization must take place in a strikingly short time. We have constructed a nondeterministic model of the processes occurring throughout an Interval or an Episode that are relevant for triggering a transition into or out of a REM sleep episode. In a sense, the notion of state is extended beyond its overt manifestations to those underlying processes that affect the dynamics of state transitions. The results of such a model can be correlated with actual physical processes thought to play critical roles in transitions between states or continuance of a given state.

Mathematical modeling has been an important driving force for conceptual systematization in the sleep field.[27-29] Long-term monitoring of REM sleep occurrence shows that the lengths of Episodes and Intervals are highly variable, a fact that has led to modeling the distribution of their lengths as the outcome of a stochastic process. Stochastic models have been proposed for the duration of W and sleep periods in human subjects and other mammalian species.[30,31] Closer to our present concern, a stochastic model of the distribution of REM sleep Episodes and Intervals in rats has been developed based on the observation that the distribution of both Episodes and Intervals follow a bimodal shape with an initial sharp peak and a second smoother increase.[13] That model is based on the observed incidence of length distributions that is fit to a mixture of 2 Poisson distributions. In the present report, rather than considering the lengths of Episodes and Intervals directly as the stochastic variables, emphasis is placed on the occurrence of transitions into and out of REM sleep, and stochasticity is associated to the occurrence of those transitions. What must be modeled are the underlying processes that, as Episodes or Intervals evolve, make more or less likely a transition. These processes can be locally modeled as Poisson processes characterized by a single parameter. The purpose of the present study has been to assess the time course of that parameter throughout an Interval or an Episode.

Permanence in behavioral states and transitions between states should involve characteristic neural and biochemical correlates. The search for neuroanatomic structures critical for state induction and continuance has been a central issue for sleep research.[3,5,32,33] The role of specific neurotransmitters was emphasized early,[34] and many neurotransmitter systems were later proposed to be involved in sleep-state regulation.[35] The search for molecular correlates of sleep, such as state-dependent gene expression,[36,37] is expected to provide a better understanding of the cellular biology that underlies state continuance and transitions. The reciprocal interaction model of REM sleep generation is based on the interplay between brainstem cholinergic REM-on neurons and aminergic REM-off neurons and on the time course of the building up of neurotransmitter effects and firing patterns.[5,38-40] The role of mutually inhibiting neural structures and ensuing flip-flop mechanisms for stabilizing and switching states has been highlighted for both sleep-wake and NREM sleep-REM sleep alternations.[1,2] Information about state-specific firing patterns from critical neural areas, particularly their time course throughout the sleep-wake cycle, becomes a most interesting issue.[33,40-46]

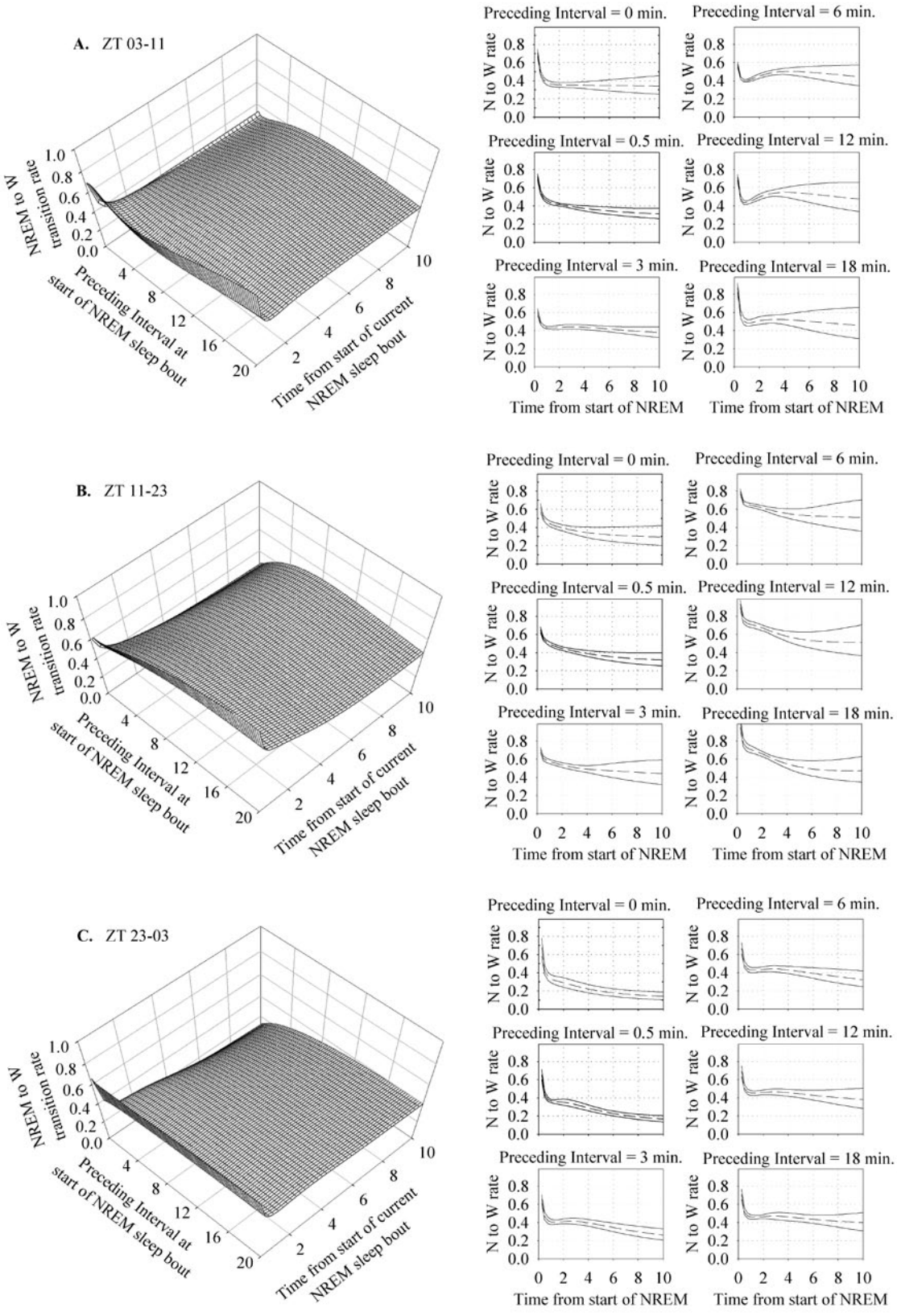

Figure 5—The 3D mesh plots correspond to time segments of 24-hour data: **A.** 03-11, **B.** 11-23 and **C.** 23-043 and display the dynamic course of the rate of transition from non-rapid eye movement (NREM) sleep to wake (W) through a given NREM sleep bout adding as a second modulating variable the time at which the NREM bout began after the Interval started. The 2D panels at the right of each 3D mesh plot are cross sections displaying the modulation of the rate of transition from NREM sleep to W as a function of time from the start of the NREM bout at 6 different times elapsed from the beginning of an Interval and the start of the NREM sleep bout being examined.

Changes in behavioral states involve a cause-effect sequence. Transitions are the result of an underlying neural and biochemical substrate, but, at the same time, after a transition occurs, the new state may determine a new neural and biochemical substrate. Neural discharge, intracellular events, and neurotransmitter concentration may change at different time scales. Part of the rationale for the present work has been to account for the coupling of abrupt changes triggered at some point by processes that may themselves undergo a slower modulation. Homeostatic and circadian processes account for the regulation of behavior states.[27] A bout of a given state involves the transition into the state, followed by a stable phase for the duration of the bout, and ending with a transition out of the state. The drive to enter, stay, and exit a given state depends as much on factors related to that state as to factors related to potentially competing ones. This is metaphorically implied in the literature by terms such as REM sleep pressure and NREM sleep pressure. By definition, a transition involves both the process of going out of a given state and the process of going into another one. Furthermore, since state transitions should involve energy-demanding reconfigurations, one may expect that many attempts will turn out to be unsuccessful, a consideration consistent with the peaks of very short Episodes and very short Intervals observed in the actual corresponding distributions. Finally, the mechanisms responsible for going into a state need not be the same with sign opposite to those responsible for going out of a state, just as hunger and satiety may involve different mechanisms.

The previous paragraph summarizes the context in which our results will now be discussed. Our model is based on the evolution of 3 variables: opportunity, propensity, and volatility. Opportunity shows a rapid ascending phase followed by a much slower descent. The ascending phase reflects a tendency to transit from REM sleep to W and then rapidly go back to NREM sleep. The ensuing decay suggests that longer intervals reflect the presence of self-stabilizing W. Propensity and volatility start at their highest level and rapidly decay to rise again, sharply in the case of volatility, and moderately in the case of propensity. Since sleep variables undergo a strong 24-hour modulation, these general features of opportunity, propensity, and volatility were analyzed throughout the 12:12 L:D schedule. The time course of opportunity is related to NREM sleep. High levels of opportunity throughout the Interval are observed in the last hour of the dark phase and first hours of the light phase, coinciding with the highest incidence of NREM sleep. Coherently, this high occurrence of NREM sleep at a time of low propensity for REM sleep keeps offering opportunities that are not being realized. Propensity and volatility display a 24-hour modulation that is particularly noticeable at the beginning of the Episode or Interval. Their curves are roughly inverted, propensity rising and volatility decreasing through the light phase. High propensity and low volatility, plus the high level of opportunity, favor REM sleep expression. This is consistent with the fact that, in the rat, the sinusoidal 24-hour distribution of REM sleep reaches its highest incidence during the second half of the rest-predominant, lights-on phase.[19,20,24] Based on these 24-hour distributions, particularly on that of opportunity, we built our databases according to the 3 time segments ZT 23-03, ZT-03-11, and ZT 11-23.

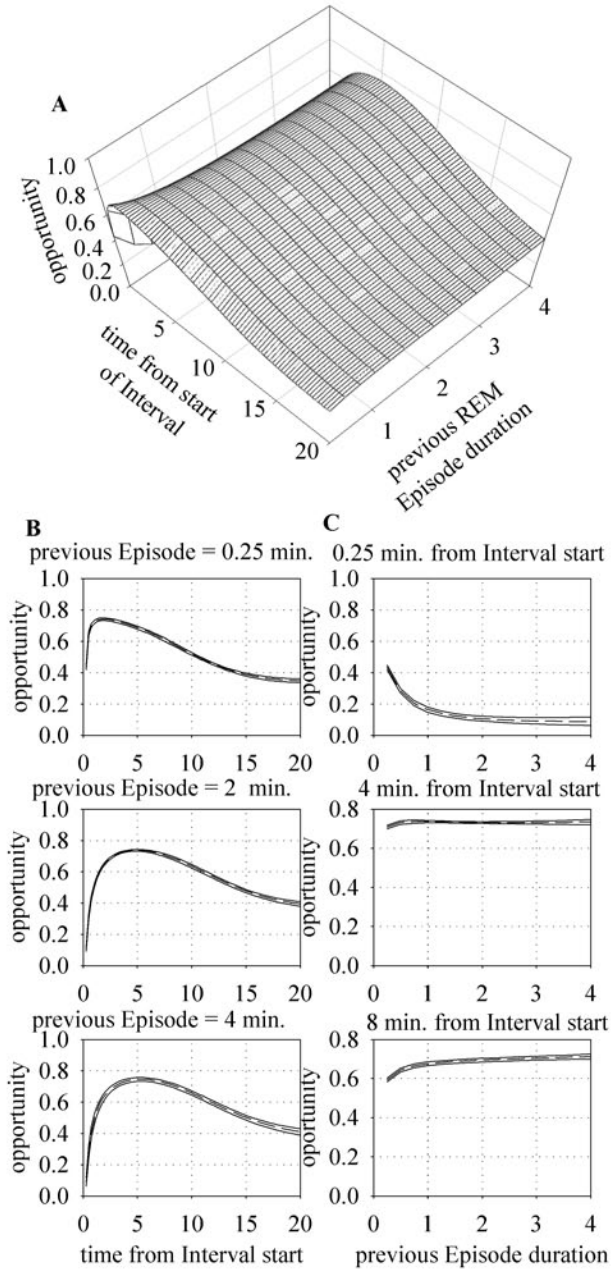

Figure 6—A. Mesh plot displaying the dynamic course of opportunity through the Interval as a function of the previous rapid eye movement (REM) sleep Episode duration. **B.** Cross sections displaying opportunity at 3 different values of previous REM sleep Episode duration. **C.** Cross sections displaying the modulation of opportunity as a function of previous REM sleep Episode duration at 3 different times from the start of the Interval. Panels in B and C show the output of the aggregated model (dashed curve) within a 1-standard deviation span (thick solid curves). Opportunity is measured as probability of being in non-rapid eye movement (NREM) sleep, a value between 0 and 1.

The initial high level of propensity and volatility can be interpreted as an inertial effect of the previous state and the subsequent rapid fall as a stabilization process of the new state. Inertia is the lingering effect of the previous substrate; stabilization is the successful take over by the new paradigm. In the case of propensity, the inertia indicates a high probability that,

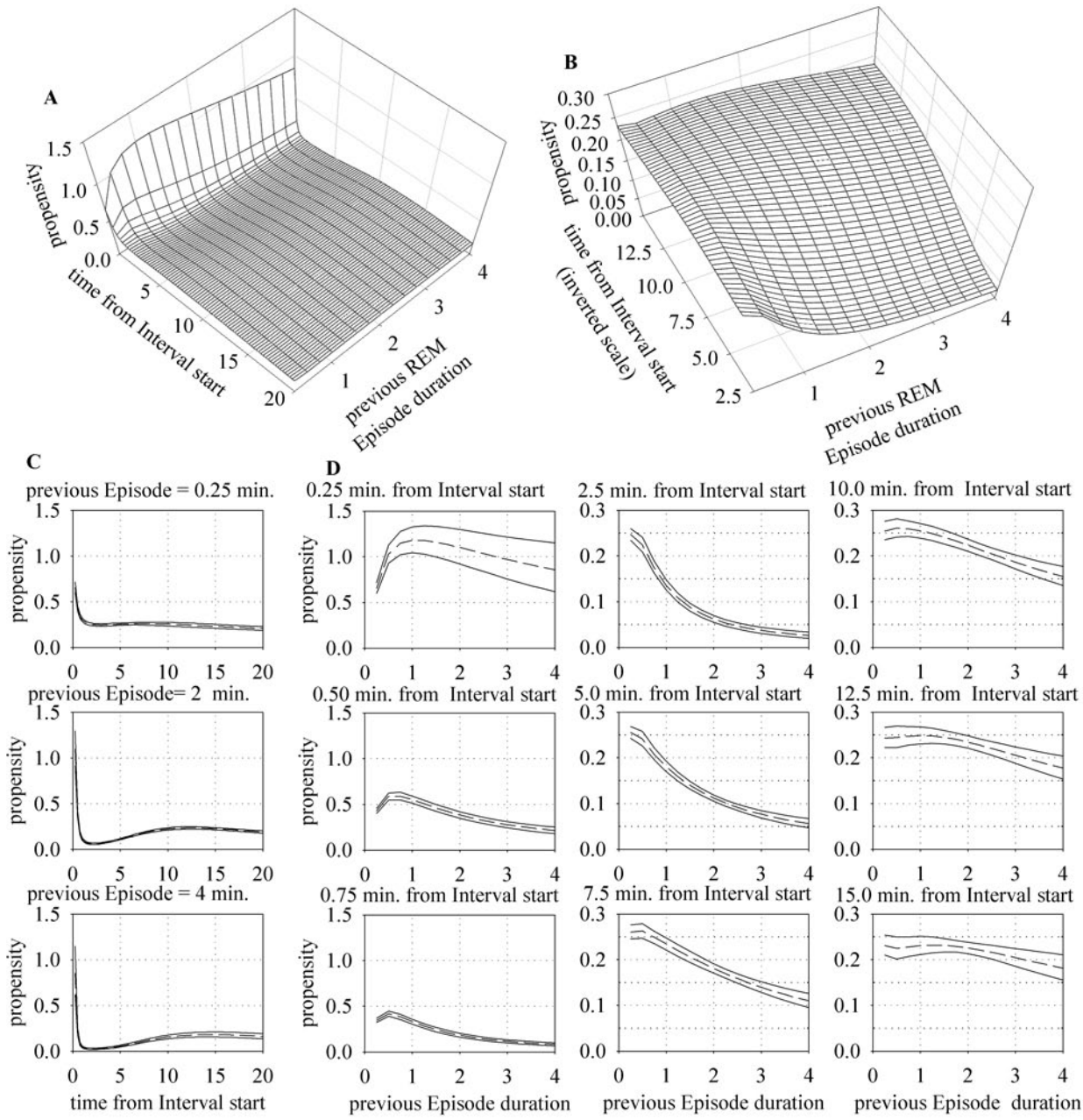

Figure 7—A. Mesh plot displaying the dynamic course of propensity through the Interval as a function of the previous rapid eye movement (REM) sleep Episode duration. **B.** Mesh plot highlighting the dynamic course of propensity from 2.5 to 15.0 minutes after the start of the Interval. Note that the propensity scale is different and that the time-after-start-of-Interval axis is inverted. **C.** Cross sections displaying propensity at 3 different values of previous REM sleep Episode duration. **D.** Cross sections displaying the modulation of propensity as a function of previous REM sleep Episode duration at 9 different times from the start of the Interval. Note that ordinates have different scales in the first 3 panels. Panels in C and D show the output of the aggregated model (dashed curve) within a 1-standard deviation span (solid curves). Propensity is measured as the rate of occurrence of into-REM transitions expressed as events per minute.

given the opportunity to go immediately back to REM sleep, it will be taken, but, if it is not, the new Interval will stabilize itself. The same can be said for volatility, since, at the beginning of the Episode, it is probable that a transition into REM sleep will not succeed, but, if it does, the state will be expected to endure. After falling from their initial high level, propensity or volatility may either stay at a low level or rise. The latter case should be interpreted as a destabilization process due either to a self-limited saturation of the current state or to an increase pressure of the alternative state. Actually, volatility conspicuously doubles its value from minute 1.0 to 3.0 after the start of the Episode, whereas, when propensity is assessed through the Interval, the rise in the tendency to enter REM sleep is much less pronounced. If the NREM sleep and W contents of the Interval are considered separately, the rise in propensity seems to be related to the NREM sleep content.

The effect of NREM sleep was better assessed by monitoring propensity through a NREM sleep bout while controlling

for total Interval time. When a NREM sleep bout starts at the very beginning of the Interval, an inertial effect is expressed by a very high initial propensity. Propensity falls as that NREM sleep bout evolves, but it remains at higher levels than the corresponding initial ones observed as the NREM sleep bout starts later into the Interval; the implication being that intervening W counteracts more effectively the REM sleep inertial effect. A second remarkable fact is the ascent of propensity after a very low initial level observed when the bout starts roughly 2 or more minutes into the Interval. This increment of propensity through the first minute of the bout illustrates the concept of REM sleep priming by NREM sleep or the need for NREM sleep to occur after W for a transition into REM sleep to be possible. After some 4 minutes into the bout, a pronounced further increase may be observed, meaning that, at least in this situation, more NREM sleep makes more likely a transition into REM. This late increase occurs only when the NREM sleep bout had started after at least 3 minutes of Interval and is not present at ZT 23-03. Actually, in that time segment, there is a decrease in propensity after the early rise just described as corresponding to the priming effect. The late propensity rise is also absent during ZT 03-11 and ZT 11-23 when the preceding Interval has been short. This fact may be explained by the proximity of the last Episode, which would lessen the drive for a new Episode during the NREM sleep bout.

Since the previous analysis examined transitions into REM sleep as a NREM sleep bout evolves, we wanted to compare it with the evolution of transition rate into W through a NREM sleep bout. The data are presented in Figure 5 and show that there is a consistent pattern of decrease after the initial high point indicative of a W into NREM sleep inertial effect. We also performed analysis, not shown in the results section, that indicated that, the longer the previous W bout, the stronger its inertial effect on the sleep to W transition rate at the beginning of a sleep bout.

REM sleep short-term homeostasis was assessed by analyzing the effect of the length of the previous Episode on propensity. That effect is straightforwardly expressed by the descent of the propensity when the previous Episode duration is longer. Short-term homeostasis can be thought of as the capacity of longer REM sleep episodes to lower the propensity curve for longer times. Furthermore, the time course of the homeostatic effect can be approximated by observing through the panels of Figure 7D how the modulation of propensity by previous Episode duration fades after minute 5 of the Interval. Note also that only in the first panel of Figure 7D is an ascending segment evidenced for short previous Episodes of up to 1.0 minute in duration. This fact can also be explained by an inertia effect, since the short intervening Episode would have been insufficient to stabilize the REM sleep state and to generate REM sleep inertia, and, consequently, the underlying substrate of the previous Interval still remains in force at the beginning of the new Interval. This fact may be related to the finding that after 24 hours of sleep deprivation in the rat, the large ensuing REM sleep increase is accompanied by a reduction in unsuccessful attempts to enter REM sleep and an increase in sustained Episodes.[12] Note also that propensity at the beginning of an Interval is highest when the previous Episode lasted between 1.0 and 2.0 minutes. This inverted U-shaped curve suggests that, at one extreme, very short Episodes are not capable of establishing a REM sleep substrate and, in the other, that very long ones may have satisfied the REM sleep need and hence weakened the propensity to go back to that state. This effect and its time course throughout the Interval are confirmed by the sequence of panels displayed in Figure 7C, in which the different starting points of the curves represent an effect on REM sleep inertia. In Figure 7C, it is also remarkable that short previ-

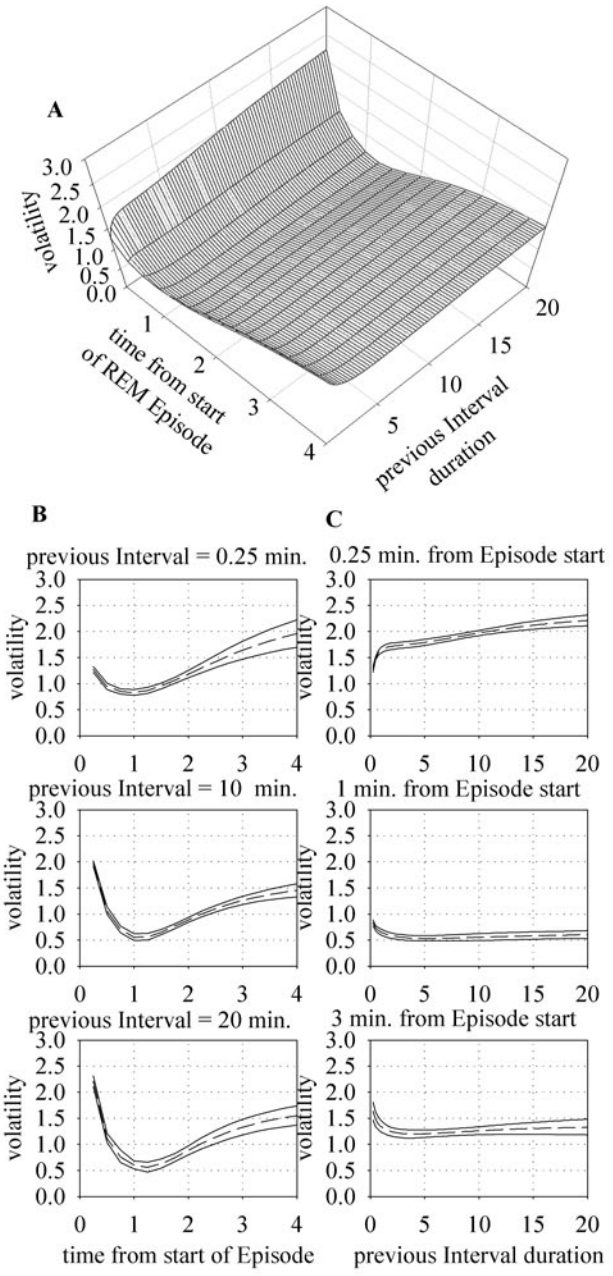

Figure 8—**A.** Mesh plot displaying the dynamic course of volatility through the rapid eye movement (REM) sleep Episode as a function of the previous Interval duration. **B.** Cross sections displaying volatility at 3 different values of previous Interval duration. **C.** Cross sections displaying the modulation of volatility as a function of previous Interval duration at 3 different times from the start of the REM sleep Episode. Panels in B and C show the output of the aggregated model (dashed curve) within a 1-standard deviation span (solid curves). Volatility is measured as the rate of occurrence of out-of-REM transitions expressed as events per minute.

ous episodes display a low starting point and a small descent in propensity, whereas longer previous episodes start with a high inertial effect followed by a large dip. A more intense and sustained dip represents the most stable phase of the Interval or a relative refractory period for REM sleep. It should also be stated that longer previous Episodes not only affect propensity but also reduce initial opportunity and delay its recovery, as observed in Figure 5. In the case of volatility, the inertial effect of the previous Interval was observed but not the homeostatic one, a fact that confirms previous reports[10] indicating that, in the basal sleep-wake cycle of the rat, the Interval length is subjected to a short-term homeostatic regulation, but the Episode length is not. Only at the very start of an Episode does volatility depend markedly on the length of the previous Interval, a fact compatible with the assumption that after very short Intervals, the system is resuming the previous Episode rather than starting a fresh new one, hence the softer stabilization and the higher saturation.

In summary, we have proposed a model that conceptualizes the stochasticity of the duration of REM sleep Episodes and Intervals as arising from continuous underlying processes that, as they evolve, set the expected rate of transitions into and out of REM sleep. Bearing such a conceptualization, we have revisited issues such as REM sleep 24-hour distribution, the effect of NREM sleep on REM sleep expression, and short-term homeostatic aspects of REM sleep regulation

ACKNOWLEDGMENTS

This work was supported by research grant Fondecyt 1060250. The authors wish to thank the reviewers for suggestions that resulted in substantial improvements to the original manuscript.

DISCLOSURE STATEMENT

This was not an industry supported study. The authors have indicated no financial conflicts of interest.

REFERENCES

1. Saper CB, Chou TC, Scammell TE. The sleep switch: hypothalamic control of sleep and wakefulness. Trends Neurosci 2001;24:726-31.
2. Lu J, Sherman D, Devor M, Saper CB. A putative flip-flop switch for control of REM sleep. Nature 2006;441:589-94.
3. Fuller PM, Saper CB, Lu J. The pontine REM switch: past and present. J Physiol 2007;584:735-41.
4. Merica H, Fortune RD. State transitions between wake and sleep, and within the ultradian cycle, with focus on the link to neuronal activity. Sleep Med Rev 2004;8:473-85.
5. Pace-Schott EF, Hobson JA. The neurobiology of sleep: genetics, cellular physiology and subcortical networks. Nat Rev Neurosci 2002;3:591-605.
6. Maquet P, Peters J, Aerts J, et al. Functional neuroanatomy of human rapid-eye-movement sleep and dreaming. Nature 1996;383:163-6.
7. Siegel JM. The stuff dreams are made of: anatomical substrates of REM sleep. Nat Neurosci 2006;9:721-2.
8. Trachsel L, Tobler I, Achermann P, Borbely AA. Sleep continuity and the REM-nonREM cycle in the rat under baseline conditions and after sleep deprivation. Physiol Behav 1991;49:575-80.
9. Amici R, Zamboni G, Perez E, et al. Pattern of desynchronized sleep during deprivation and recovery induced in the rat by changes in ambient temperature. J Sleep Res 1994;3:250-6.
10. Vivaldi EA, Ocampo A, Wyneken U, Roncagliolo M, Zapata AM. Short-term homeostasis of active sleep and the architecture of sleep in the rat. J Neurophysiol 1994;72:1745-55.
11. Barbato G, Barker C, Bender C, Wehr TA. Spontaneous sleep interruptions during extended nights. Relationships with NREM and REM sleep phases and effects on REM sleep regulation. Clin Neurophysiol 2002;113:892-900.
12. Franken P. Long-term vs. short-term processes regulating REM sleep. J Sleep Res 2002;11:17-28.
13. Gregory GG, Cabeza R. A two-state stochastic model of REM sleep architecture in the rat. J Neurophysiol 2002;88:2589-97.
14. Clark VA. Survival distribution. Annu Rev Biophys Bioeng 1975;4:431-48.
15. Kodlin D. A new response time distribution. Biometrics 1967;23:227-39.
16. Ursin R. Sleep stage relations within the sleep cycles of the cat. Brain Res 1970;20:91-7.
17. Benington JH, Heller HC. REM-sleep timing is controlled homeostatically by accumulation of REM-sleep propensity in non-REM sleep. Am J Physiol 1994;266:R1992-2000.
18. Barbato G, Wehr TA. Homeostatic regulation of REM sleep in humans during extended sleep. Sleep 1998;21:267-76.
19. Trachsel L, Tobler I, Borbely AA. Sleep regulation in rats: effects of sleep deprivation, light, and circadian phase. Am J Physiol 1986;251:R1037-44.
20. Vivaldi EA, Wyneken U, Roncagliolo M, Ocampo A, Zapata AM. Measures of location and dispersion of sleep state distributions within the circular frame of a 12:12 light: dark schedule in the rat. Sleep 1994;17:208-19.
21. Vivaldi EA, Pastel RH, Fernstrom JD, Hobson JA. Long term stability of rat sleep quantified by microcomputer analysis. Electroencephalogr Clin Neurophysiol 1984;58:253-65.
22. Roncagliolo M, Vivaldi EA. Time course of rat sleep variables assessed by a microcomputer-generated data base. Brain Res Bull 1991;27:573-80.
23. Vivaldi EA, Bassi A. Frequency domain analysis of sleep EEG for visualization and automated state detection. Conf Proc IEEE Eng Med Biol Soc 2006;1:3740-3.
24. Borbely AA. Effects of light and circadian rhythm on the occurrence of REM sleep in the rat. Sleep 1980;2:289-98.
25. Vivaldi EA, Ocampo-Garces A, Villegas R. Short-term homeostasis of REM sleep throughout a 12:12 light:dark schedule in the rat. Sleep 2005;28:931-43.
26. Breiman L. Bagging predictors. Machine Learning 1996;33:105–39.
27. Borbely AA. A two process model of sleep regulation. Hum Neurobiol 1982;1:195-204.
28. Kronauer RE, Gunzelmann G, Van Dongen HP, Doyle FJ, 3rd, Klerman EB. Uncovering physiologic mechanisms of circadian rhythms and sleep/wake regulation through mathematical modeling. J Biol Rhythms 2007;22:233-45.
29. Nakao M, Karashima A, Katayama N. Mathematical models of regulatory mechanisms of sleep-wake rhythms. Cell Mol Life Sci 2007;64:1236-43.
30. Lo CC, Amaral LAN, Havlin S, et al. Dynamics of sleep-wake transitions during sleep. EPL (Europhysics Letters) 2002:625.
31. Lo CC, Chou T, Penzel T, et al. Common scale-invariant patterns of sleep-wake transitions across mammalian species. Proc Natl Acad Sci USA 2004;101:17545-8.
32. Saper CB, Scammell TE, Lu J. Hypothalamic regulation of sleep and circadian rhythms. Nature 2005;437:1257-63.
33. Tamakawa Y, Karashima A, Koyama Y, Katayama N, Nakao M. A

quartet neural system model orchestrating sleep and wakefulness mechanisms. J Neurophysiol 2006;95:2055-69.
34. Jouvet M. The role of monoamines and acetylcholine-containing neurons in the regulation of the sleep-waking cycle. Ergeb Physiol 1972;64:166-307.
35. Siegel JM. The neurotransmitters of sleep. J Clin Psychiatry 2004;65 Suppl 16:4-7.
36. Cirelli C, Pompeiano M, Tononi G. Neuronal gene expression in the waking state: a role for the locus coeruleus. Science 1996;274:1211-5.
37. Tononi G, Cirelli C. Modulation of brain gene expression during sleep and wakefulness: a review of recent findings. Neuropsychopharmacology 2001;25:S28-35.
38. Hobson JA, McCarley RW, Wyzinski PW. Sleep cycle oscillation: reciprocal discharge by two brainstem neuronal groups. Science 1975;189:55-8.
39. McCarley RW, Hobson JA. Neuronal excitability modulation over the sleep cycle: a structural and mathematical model. Science 1975;189:58-60.
40. Lydic R, McCarley RW, Hobson JA. The time-course of dorsal raphe discharge, PGO waves, and muscle tone averaged across multiple sleep cycles. Brain Res 1983;274:365-70.
41. Hobson JA, McCarley RW, Freedman R, Pivik RT. Time course of discharge rate changes by cat pontine brain stem neurons during sleep cycle. J Neurophysiol 1974;37:1297-309.
42. Steriade M, Datta S, Pare D, Oakson G, Curro Dossi RC. Neuronal activities in brain-stem cholinergic nuclei related to tonic activation processes in thalamocortical systems. J Neurosci 1990;10:2541-59.
43. Blumberg MS, Seelke AM, Lowen SB, Karlsson KA. Dynamics of sleep-wake cyclicity in developing rats. Proc Natl Acad Sci U S A 2005;102:14860-4.
44. Takahashi K, Lin JS, Sakai K. Neuronal activity of histaminergic tuberomammillary neurons during wake-sleep states in the mouse. J Neurosci 2006;26:10292-8.
45. Behn CG, Brown EN, Scammell TE, Kopell NJ. Mathematical model of network dynamics governing mouse sleep-wake behavior. J Neurophysiol 2007;97:3828-40.
46. Best J, Diniz Behn C, Poe GR, Booth V. Neuronal models for sleep-wake regulation and synaptic reorganization in the sleeping hippocampus. J Biol Rhythms 2007;22:220-32.